Quantum rings under magnetic fields: Electronic and optical properties

Z. Barticevic,[1] M. Pacheco,[2,*] and A. Latgé[3]
[1]*Departamento de Física, Universidad Técnica F. Santa María, Casilla 110-V, Valparaíso, Chile*
[2]*Departamento de Física, Universidad de Santiago de Chile, Casilla 307, Santiago, Chile*
[3]*Instituto de Física, Universidade Federal Fluminense, Av. Litorânea s/n, 24210-340 Niterói-RJ, Brazil*
(Received 20 January 1999; revised manuscript received 21 March 2000)

Electronic and optical characteristic energies of semiconductor quantum rings in the presence of magnetic fields were determined by adopting distinct potential models to describe the ring confinement and considering different geometric confinement parameters defining the quantum ring. It was found that the ground-state energy becomes independent of the ring radius once the internal ring hole is present, because it is the strength of the lateral confinement that determines its subsequent behavior. The optical spectra for large and narrow quantum rings exhibit a set of resonances governed basically by the strength of the radial confinement. The presence of a magnetic field produces a notable enhancement of the resonance intensities.

Increased development of semiconducting growth technology makes possible the fabrication of very small nanostructures exhibiting high quantum confinement. As its electronic states present a complete discrete nature, they can be viewed as natural candidates for optoelectronic devices and a large number of work has been done on semiconductor heterostructures of reduced dimensions.[1] Recently, nanostructures similar to rings in reduced scale were grown via high-resolution electron-beam lithography techniques[2] and have been characterized by low-temperature photoluminescence measurements. On the other hand, quantum rings (QR's) are natural systems to study quantum interference phenomenon in transport properties. Actually, a metallic ring of mesoscopic dimension in an external magnetic field exhibits an equilibrium current which is periodic in the Aharanov-Bohm flux.[3–5] The magnetic response of a GaAs/$Ga_xAl_{1-x}As$ mesoscopic ring was experimentally reported[6] with a periodic signal which is the signature of a persistent current. Also, the effects of electron-electron interaction on the persistent current in a mesoscopic QR subjected to a magnetic field was discussed by Chakraborty and Pietilainen[7] and theoretical studies on the optical-absorption spectra have been presented by Halonen *et al.*,[8] taking into account repulsive scattering centers.

Motivated by a wide variety of interesting physical phenomena in QR's we present here a theoretical study of electronic and optical properties of these low-dimensional systems. The energy spectrum of the QR is calculated within the effective-mass approximation, including the effect of an external magnetic field applied in the axial direction of the ring and neglecting excitonic effects and the presence of impurities. Quantum rings can be theoretically modeled by the superposition of two confining potentials: One in the z direction, defined by the growth of GaAs and $Ga_xAl_{1-x}As$ layers, and other in the lateral direction. The adequate choice for modeling this last potential should be guided by the experimental growth techniques used to achieve the ring geometry. Two models for the lateral ring confining potential are discussed: a cylindrical parabolic potential (CPP) that is more suitable for etched heterostructures, and a cylindrical square-well potential (SWP) that is appropriate for describing heterostructures immersed in a semiconductor matrix. The system results in a model very similar to a cylindrical quantum dot[9] (QD), except for the internal cavity of the ring which guarantees a stronger radial confinement than the corresponding one defined by a QD of the same size.

The effective-mass Hamiltonian describing an electron in a quantum ring, under the presence of a magnetic field B applied in the axial direction, can be written as

$$H=\frac{1}{2m^*}\left(\vec{p}+\frac{|e|}{c}\vec{A}\right)^2+V_{qw}(z)+V_{Lat}(\rho), \tag{1}$$

with $\vec{A}$ being the vector potential and m^* the electron effective mass. We have modeled the QR by a square-well potential in the z direction, $V_{qw}(z)$, and a lateral confinement potential $V_{Lat}(\rho)$, where ρ is the in-plane coordinate. This last potential has been chosen as a square-well potential (SWP), given by $V_{Lat}(\rho)=0$, if $\rho_1 \leqslant \rho \leqslant \rho_1+\rho_{qw}$, and equal to V_ρ otherwise, ρ_1 being the internal radius of the ring and ρ_{qw} the length of the lateral quantum well, and a cylindrical parabolic potential (CPP), given by $V_{Lat}(\rho)=\frac{1}{2}m^*\omega_g^2(\rho-\rho_{ring})^2$, with ρ_{ring} being the center of the parabolic confinement potential and ω_g the geometric frequency that determines the strength of the ring lateral confinement. This confinement is measured through the parameter $\rho_{conf}=\sqrt{\hbar/m^*\omega_g}$ which corresponds, in the case of a bidimensional harmonic oscillator, to the ground-state expectation value of the lateral coordinate.

The electronic envelope wave function, solution of the eigenvalue problem defined by the Hamiltonian in Eq. (1), can be written as $\Psi_{nl}(z,\rho,\varphi)=\Phi_n(z)R_l(\rho,\varphi)$, l being the orbital quantum number and $\Phi_n(z)$ the quantum-well solutions along the z direction. The functions $R_l(\rho,\varphi)$ are the solutions of the lateral eigenvalue problem

$$H_{lat}R_l(\rho,\varphi)=E_{lat}R_l(\rho,\varphi). \tag{2}$$

In the following we discuss the two model potential calculations.

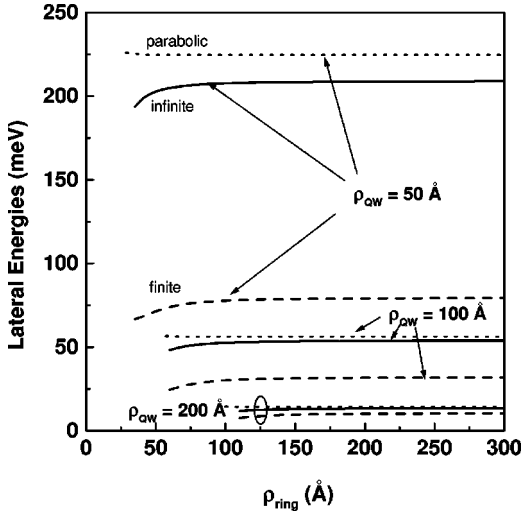

FIG. 1. Lateral electron energies for a GaAs/$Ga_xAl_{1-x}As$ QR as a function of the ring radius for different values of ρ_{qw}. Full and dashed curves correspond to the infinite and finite square-well model, respectively, whereas the dotted lines denote the results following the parabolic model.

SQUARE WELL POTENTIAL AND $B=0$

Taking into account the asymptotic behavior of the wave function in the QR interfaces, the solutions of the eigenvalue problem of Eq. (2) are given by $R_l(\rho)=r_l(\rho)e^{il\varphi}$, with

$$r_l(\rho)=\begin{cases} C_l I_l(\rho\beta_1) & \text{if } \rho\leqslant\rho_1 \\ A_l J_l(\rho\beta_0)+B_l Y_l(\rho\beta_0) & \text{if } \rho_1\leqslant\rho\leqslant\rho_2 \\ D_l K_l(\rho\beta_1) & \text{if } \rho\geqslant\rho_2, \end{cases} \quad (3)$$

where $\rho_2=\rho_1+\rho_{qw}$, J_l and Y_l, are Bessel functions, whereas I_l and K_l are modified Bessel functions of the lth order. The parameter β_o (β_1) is defined by $(2m^*E_{lat}/\hbar^2)^{1/2}$ ($[2m^*(V_\rho-E_{lat})/\hbar^2]^{1/2}$). The energies are obtained by solving the transcendental equations which results from applying standard boundary conditions for the wave functions defined in Eq. (3).

CYLINDRICAL PARABOLIC POTENTIAL AND $B\neq0$

In this case a magnetic field applied in the axial direction is considered. Choosing the symmetric gauge for $\vec{A}$ in the effective-mass Hamiltonian [Eq. (1)] we have

$$H_{lat}=-\frac{\hbar^2}{2m^*}\nabla_\rho^2+\frac{\hbar\omega_c}{2}l+\frac{1}{2}m^*\omega_{eff}^2(\rho-\rho_0)^2 + \frac{1}{8}m^*\omega_{eff}^2\frac{\omega_c^2}{\omega_g^2}\rho_0^2, \quad (4)$$

where $\omega_c=eB/m^*c$ is the cyclotron frequency, ω_{eff} is an effective frequency given by $\omega_{eff}=(\omega_g^2+\omega_c^2/4)^{1/2}$, and $\rho_0=(\omega_g^2/\omega_{eff}^2)\rho_{ring}$. To solve the eigenvalue problem we expand the lateral function $R_l(\rho,\varphi)$ in a linear combination of Gaussian functions[9] centered in ρ_0 and defined by different values of the standard deviation parameter,

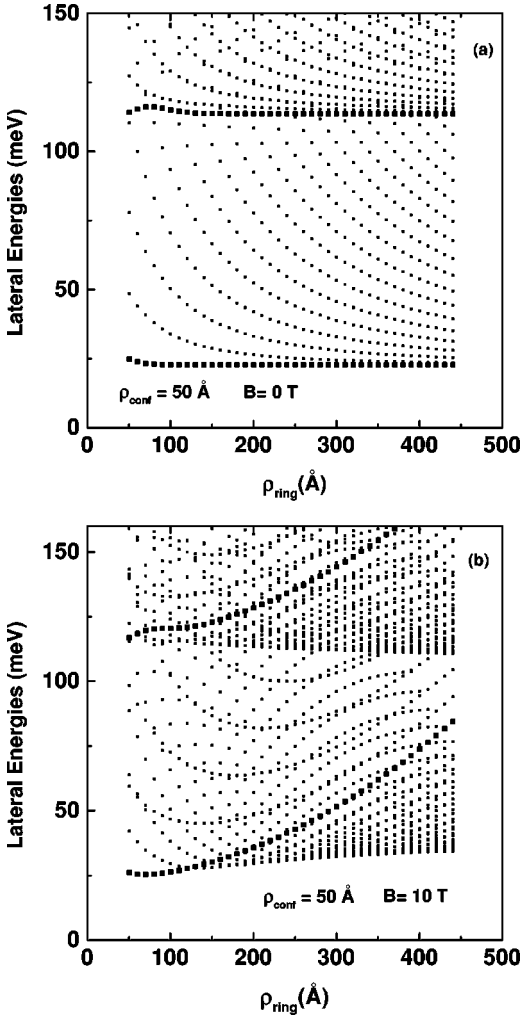

FIG. 2. Electronic lateral spectrum of a QR as a function of the ring radius using the CPP model for $\rho_{conf}=50$ Å and for (a) $B=0$ and (b) $B=10$ T. The $l=0$ state is shown by dark squares.

$$R_l(\rho,\varphi)=e^{il\varphi}\sum_m A_m^l\rho^{|l|}e^{-(\rho-\rho_0)^2/\lambda_m}. \quad (5)$$

The set of λ_m parameters is fixed *a priori* to cover the physical range of relevant radii associated with the lateral confinement. The maximum (minimum) value of this set of parameters was taken as being two order of magnitude larger (lower) than the value of those characteristic lengths. This method allows us to obtain simultaneously the ground and excited states and the convergence of each state is controled by varying the number of Gaussian functions in the expansion. To obtain accurate energies and wave functions we have used a maximum set of 26 Gaussians. The problem reduces then to solve a set of coupled homogeneous linear equations for the coefficients of the expansion A_m^l, given by

$$\sum_m A_m^l N_{mm'}^l\Big[[\beta_{mm}\beta_{m'm'}+1][D_{-2|l|}(\alpha)+D_{-2(|l|+1)}(\alpha)] - 2\beta_{mm'}\Big[2E_{Lat}-\hbar\omega_c l-\frac{m^*}{4}\omega'^2_c\rho_0^2\Big] \times D_{-2(|l|+1)}(\alpha)\Big]=0, \quad (6)$$

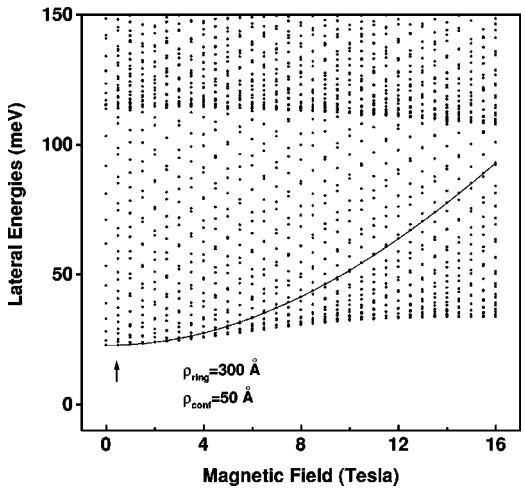

FIG. 3. Magnetic-field dependence of the electronic spectrum of a QR with $\rho_{ring}=300$ Å and $\rho_{conf}=50$ Å. The continuous line shows the state $l=0$.

with $\beta_{mm'}=1/\lambda_m+1/\lambda_{m'}$, $\alpha=-\rho_0\sqrt{2\beta_{mm'}}$, $\omega_c'=\omega_c\omega_{eff}/\omega_G$, $N^l_{mm'}$ being the normalization factors, and D_l the first-order parabolic cylindrical function.

The interband absorption spectra are obtained by calculating the transition probability per unit time for transitions from hole to electron states, following the dipolar approximation, and neglecting excitonic effects. For the case of holes, an in-plane ($0.1m_0$) and a z-direction ($0.377m_0$) effective mass are considered whereas for electrons we have used $m^*=0.0667m_0$ (m_0 being the free-electron mass). Lorentzian curves of width 2.0 meV were adopted in the absorption coefficient calculation to take into account thermal and other scattering effects.

A first analysis of the lateral electron energies of QR's with different internal radius adopting the SWP model indicates the characteristic $1/\rho_{qw}^2$ feature, a typical effect of the quantum confinement. As expected, the energies reach limit values exhibiting the behavior of rectangular and cylindrical quantum wires as the internal radius increases and decreases, respectively. The electronic energies of GaAs/Ga_xAl_{1-x}As QR's with different lateral confinement and for $l=0$ are shown in Fig. 1 as functions of the mean ring radius ρ_{ring}. Different cylindrical ring potential models were used: finite (for GaAs/$Ga_{0.67}Al_{0.33}$As) and infinite square wells and the parabolic one. The confinement parameters for the SWP model, (ρ_1,ρ_{qw}), and the CPP model, $(\rho_{ring},\rho_{conf})$, are related via the following expressions: $\rho_{ring}=\rho_1+\rho_{qw}/2$ and $\rho_{conf}=\rho_{qw}/\pi$, the last equivalence coming from the standard relation between the lengths associated with a harmonic potential and an infinite square-well potential. It should be noted that the energies do not depend on the particular ring radius except for rings with small internal radius. In this regime, however, the energies exhibit an opposite behavior for the different adopted models. In the SWP model the lateral energies decrease, indicating a transition to a lower confinement regime. In this limit the QR becomes a cylindrical QD, and for that model the lateral confinement is now $2\rho_{qw}$. On the other hand, for $\rho_{ring}=0$ in the parabolic model, one gets a double-confined QD. It also can be noticed that for all considered values of the lateral-confinement, the finite barrier square-well model yields lower lateral energies than the infinite well and parabolic models; a finite barrier potential imposes a limit for the energy value of the bound states in the well. Moreover, in the high confinement regime, for $\rho_{qw}=50$ Å, the large differences between the lateral energies obtained by using infinite models and a finite potential indicates that an adequate choice of the potential must take into account the conditions under which the annular confinement is achieved.

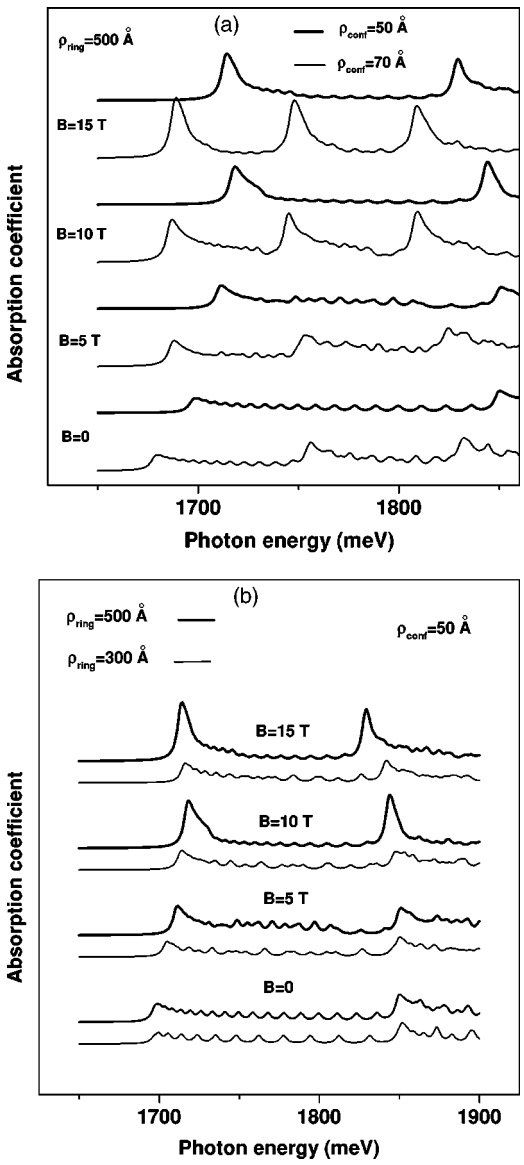

FIG. 4. Optical spectra of a GaAs/Ga_xAl_{1-x}As QR for magnetic fields up to 15 T. In (a) $\rho_{ring}=500$ Å and $\rho_{conf}=50$ Å (bold lines) and 70 Å (light curves) and in (b) $\rho_{conf}=50$ Å and $\rho_{ring}=300$ Å (light curves) and 500 Å (bold lines).

In what follows the effects of applied magnetic fields on the lateral energies of GaAs QR's are analyzed using the *parabolic model*. The results presented in Figs. 2(a) and 2(b) show the dependence of the lateral energies on the ring radius, for a ring confinement of $\rho_{conf}=50$ Å, and for $B=0$ and $B=10$ T, respectively. In the *quantum dot* limit ($\rho_{ring}=0$) the energy spectrum is expected to exhibit two essential features: the energy difference between the lowest two $l=0$ levels (marked with large black squares in the figure)

should correspond to $2\hbar\omega_g$ while the minimum energy difference between two states would be given by $\hbar\omega_g$, which occurs for momentum angular values differing by unity. For increasing values of the QR radius the energy spectrum almost preserves the mentioned energy separation of $2\hbar\omega_g$ for the marked $l=0$ levels but other solutions appear between then, reducing the corresponding energetic spacing and enlarging the density of energy levels in the spectrum. In the limit of very large ring radius as compared with the ring width ($\rho_{ring} \gg \rho_{conf}$) it is possible to treat the problem as the superposition of a one-dimensional parabolic potential, with a confinement parameter given by ρ_{conf} and an infinite well potential of width $L=2\pi\rho_{ring}$.

In the presence of a magnetic field the spectrum changes drastically [see Fig. 2(b)]. The magnetic field breaks the degeneracy between the states with positive and negative angular momentum and the ground state becomes a state with $l \leqslant 0$, depending on the confinement ring parameters. This can be understood considering the limit of an ideally narrow ring for which $\rho_{conf} \to 0$ and the eigenvalues are given by[7] $E=(\hbar^2/2m^*\rho_{ring}^2)[l+(\rho_{ring}^2/2\rho_L^2)^2$, $\rho_L^2=\hbar c/eB$ being the Landau radius. A more complex spectrum is obtained for a finite-width ring due to the presence of the levels associated with the lateral degree of freedom. Similarly to the case of $B=0$ for $\rho_{ring} \gg \rho_{conf}$ the energy spectrum is essentially given by a superposition of the energy levels of a one-dimensional ring under a magnetic field, and the energy levels associated with the radial confinement. The most remarkable feature is the accumulation of the energy levels near those states. This property of the density of states greatly influences the optical behavior of QR's as will be shown below. The same characteristic behavior discussed above is exhibited by the energy spectrum as a function of the magnetic field as shown in Fig. 3, for a $\rho_{ring}=300$ Å and $\rho_{conf}=50$ Å where the $l=0$ state is shown by the continuous line. The lifting of the degeneracy is clearly exhibited in the energy spectrum in the presence of a nonzero magnetic field which is marked by an arrow in the figure.

The interband absorption spectra of distinct quantum rings modeled by the cylindrical parabolic potential are shown in Figs. 4(a) and 4(b), for magnetic fields up to 15 T. The *z*-direction confinement was described by a quantum-well potential of width equal to 40 Å. Figure 4(a) displays different spectra for QR's defined by $\rho_{ring}=500$ Å and two different lateral confinement given by $\rho_{conf}=50$ Å (bold lines) and 70 Å (light curves). In the absence of a magnetic field the energy separation between the two main peaks for the ring of width 50 Å is twice the corresponding one for the 70-Å ring, reflecting a $1/\rho_{conf}^2$ dependence. For each spectrum, the position of the main resonances are basically determined by the lateral confinement being almost independent of the ring radius as can be seen in Fig. 4(b) where the results for the absorption coefficient for rings of two different radii, and for a fixed value of the radial confinement are shown. It can be noticed in both figures an enhancement of the optical resonances as the magnetic field increases, this effect being more pronounced for a large radius ring. Optical experimental measurements on quantum rings under applied magnetic fields may certainly be used for determining the geometrical characteristic of QR's.

In summary, the electronic energy spectrum has been studied as a function of different parameters defining the QR geometric confinement. In the high lateral-confinement regime, the results show a strong dependence on the potential model adopted, indicating the importance of taking into account the conditions under which the annular confinement was achieved for an adequate choice of the model. We have found that in the case of very narrow QR's with large radius the energy levels in the spectrum accumulate near those energy states mainly defined by the potential associated with the radial confinement. Moreover, the presence of an axial magnetic field increases the ring lateral confinement, providing a very structured density of states. As a consequence, large and narrow QR's present optical spectra governed mainly by the strength of the lateral confinement exhibiting well-defined resonances which are clearly enhanced for increasing magnetic fields. These are quite interesting results since it might be possible to obtain characteristic spectra of highly confined systems, like QDs, by means of these rather mesoscopic systems. Taking into account the increasing number of nanostructure growth techniques, and considering the interesting transport and optical properties that QRs exhibit, we believe the present theoretical study helps us to better understand the electronic and optical properties of those systems and their future optical-electronic applications.

ACKNOWLEDGMENTS

This work was partially supported by Fondo Nacional de Ciencias, Grant No. 1970119 and No. 1990271, by Univ. F. Santa Maria, Grant No. 991111, by Univ. de Santiago de Chile, Grant No. 049631 PD, by Fundacion Antorches/Vitae/Andes, Grant A-13562/1-3, and by CNPq.

*Electronic address: mpacheco@lauca.usach.cl

[1] F. Ribeiro, A. Latgè, M. Pacheco, and Z. Barticevic, J. Appl. Phys. **82**, 270 (1997); M. Pacheco and Z. Barticevic, J. Phys.: Condens. Matter **2**, 1079 (1999).

[2] G. E. Philipp, J. A. Mejia Galena, C. Cassou, P. D. Wang, C. Guasch, B. Vögele, M. C. Holland, and C. M. Sotomayor-Torres, in *Diagnostic Techniques for Semiconductor Materials Processing II*, edited by S. W. Pang, O. J. Glembocki, F. H. Pollak, F. Celli, and C. M. Sotomayor-Torres, MRS Symposia Proceedings No. 406 (Materials Research Society, Pittsburgh, 1996), p. 307.

[3] L. P. Levy, G. Dolan, J. Dunsmuir, and H. Bouchiat, Phys. Rev. Lett. **64**, 2074 (1990).

[4] V. Chandrasekhar, R. A. Webb, M. J. Brady, M. B. Ketchen, W.J. Gallagher, and A. Kleinsasser, Phys. Rev. Lett. **67**, 3578 (1991).

[5] Y. Aharanov and D. Bohm, Phys. Rev. **115**, 485 (1959).

[6] D. Mailly, C. Chapelier, and A. Benoit, Phys. Rev. Lett. **70**, 2020 (1993).

[7] T. Chakraborty and P. Pietilainen, Phys. Rev. B **50**, 8460 (1994); **52**, 1932 (1995).

[8] V. Hallonen, P. Pietilainem, and T. Chakraborty, Europhys. Lett. **33**, 377 (1996).

[9] Z. Barticevic and M. Pacheco, Phys. Low-Dimens. Struct. **10/11**, 249 (1995); M. Pacheco and Z. Barticevic, Phys. Rev. B **55**, 10 688 (1997).